

# Determination of galaxy photometric redshifts using Conditional Generative Adversarial Networks (CGANs)

M. Garcia-Fernandez<sup>1a</sup>

*<sup>a</sup>School of Architecture, Engineering and Design, Universidad Europea de Madrid, Calle Tajo s/n, Villaviciosa de Odon, 28670, Madrid, Spain*

---

## Abstract

Accurate and reliable photometric redshifts determination is one of the key aspects for wide-field photometric surveys. Determination of photometric redshift for galaxies, has been traditionally solved by use of machine-learning and artificial intelligence techniques trained on a calibration sample of galaxies, where both photometry and spectrometry are determined. On this paper, we present a new algorithmic approach for determining photometric redshifts of galaxies using Conditional Generative Adversarial Networks (CGANs). Proposed CGAN implementation, approaches photometric redshift determination as a probabilistic regression, where instead of determining a single value for the estimated redshift of the galaxy, a full probability density is computed. The methodology proposed, is tested with data from Dark Energy Survey (DES) Y1 data and compared with other existing algorithm such as a Random Forest regressor.

*Keywords:* Conditional Generative Adversarial Networks, photometric-redshift, galaxy-surveys

---

## 1. Introduction

Wide-field photometric surveys have been a major source for experimental results for Observational Cosmology. Among many of the present and future

---

<sup>1</sup>manuel.garcia2@universidadeuropea.es

photometric surveys we can find: DES<sup>2</sup>, LSST<sup>3</sup>, PAU<sup>4</sup>, J-PAS<sup>5</sup> and Euclid<sup>6</sup>. One of the key aspects of wide-field photometric surveys is the reliable determination of the redshift of the galaxies. At photometric surveys, the redshift of galaxy spectra is inferred by measuring the brightness of galaxies at broad-band filters instead of determining the Doppler shift of their spectra with a high-resolution spectrometer.

The usual approach for translating from the brightness measured at the broad-band filters to a redshift that is the closest as possible to the potential actual spectroscopic redshift, the use of machine-learning and artificial intelligence techniques are used. These techniques, make use of a calibration sample of galaxies with known both the photometry and the high-resolution spectra. This calibration sample, is used by the machine-learning algorithms as a source for identifying and discovering patterns relating the brightness at the different broad-band filters with the spectroscopic redshift.

Previous machine-learning algorithms for photometric redshift determination have included: template-fitting (Schaap and van de Weygaert, 2000; Bolzonella et al., 2011; Benítez, 2011; Arnouts and Ilbert, 2011; Laur et al., 2022), neural networks (Collister and Lahav, 2004; Sadeh et al., 2016; Mahmud Pathi et al., 2024; Hoyle, 2016; Chunduri and Mahesh, 2023; Carrasco Kind and Brunner, 2013; Almosallam et al., 2016; Cavuoti et al., 2017), boosted decision trees (Gerdes et al., 2010)-, convolutional neural networks (D’Isanto and Polsterer, 2018; Schuldt et al., 2021), bayesian neural networks (Lima et al., 2022), random forest (Lu et al., 2023), recurrent neural networks (Luo et al., 2024) and nearest neighbours (Graham et al., 2018). A good systematic review on the different types of photometric redshift algorithms can be found at Sánchez et al. (2014); Salvato et al. (2019) and Newman and Gruen (2022).

As it can be identified at literature review, the most widely used machine-learning technique at photometric redshift estimation are neural networks at their many flavours (dense, recurrent and convolutional), with a strong presence of feed-forward neural networks composed by dense layers. Feed-forward neural networks composed by dense layers are a great computational tech-

---

<sup>2</sup><https://www.darkenergysurvey.org>

<sup>3</sup><https://www.lsst.org>

<sup>4</sup><https://pausurvey.org>

<sup>5</sup><https://www.j-pas.org>

<sup>6</sup><https://www.euclid-ec.org>

nique for solving the photometric redshift estimation task, as they constitute an excellent regression technique for multivariate analysis that -if provided a proper loss function-, can minimize the errors between the inferred redshift and the actual spectroscopic redshift of the calibration sample without the need for providing an explicit functional dependence between, template or prior assumption (Bishop, 2006; Goodfellow et al., 2016). Nevertheless, the estimation of these photometric redshifts constitute a point estimate of the spectroscopic redshift instead of a probability density function. A good point estimate is necessary for some cosmological probes -such as Baryon Acoustic Oscillation (Crocco et al., 2018)-, but for other cosmological probes require to have a good control of the tails of the probability distribution function -such as number-counts magnification (Garcia-Fernandez et al., 2018)-.

A new class of neural network that has still not been explored at photometric redshift estimation are the Generative Adversarial Networks (GANs). GANs (Goodfellow et al., 2014), are a set of two neural networks, a Generator network and a Discriminator network that compete between each other. The Generator aims to generate synthetic data mimicking the real data, whereas the Discriminator network aims to identify if a given data-record is synthetic data produced by the Generator or is an observation of the real data. On the process of training this algorithm, both Generator and Discriminator compete with each other in a zero-sum competitive game approach, that is finished when the Generator can completely fool the Discriminator, so the Discriminator is not able to properly disentangle synthetic data from real data. As a consequence of this, the Generator network can accurately map the full probability distribution of the underlying data without the need of providing any prior assumption or template.

A very relevant special case for GANs, are the Conditional Generative Adversarial Networks (CGANs), which instead of tracing the full probability density function of the underlying data, they trace the conditional probability density function, provided some input condition (Mirza and Osindero, 2014).

On this paper, we propose the use of CGANs for estimating photometric redshifts using the magnitudes measured at broad-band filters. Proposed algorithm is tested with data from the Dark Energy Survey Y1 data that is overlapping with SDSS Stripe-82. Results obtained by proposed CGAN are compared with a classic machine-learning technique such as a Random Forest regressor.

## 2. Methodology

Let  $\mathbf{x}_i$  be a sample of photometric data from magnitudes measured at broad-band pass filters for the  $i$ -th galaxy of some data and  $y_i$  its corresponding known spectroscopic redshift, such that  $\{(\mathbf{x}_i, y_i)\}_{i=1}^{N_{train}}$  constitutes the data training set. Let  $\mathbf{z}_i$  be a vector of randomly-generated numbers<sup>7</sup>, associated to the  $i$ -th galaxy.

The generator network  $G$  constitutes a function such that  $\hat{y}_i = G(\mathbf{z}_i|\mathbf{x}_i; \theta_G)$ , where  $\hat{y}_i$  is the estimated photometric redshift for the set of magnitudes  $\mathbf{x}_i$  and  $\theta_G$  are the weights defining the generator neural network. On the other side, the discriminator network  $D$  provides a function such that  $d_i = D(\hat{y}_i; \theta_D)$  -with  $d_i \in [0, 1]$ - is a classifier that identifies if  $\hat{y}_i$  is a real data from the training sample or a synthetic-generated data produced by the generator network and  $\theta_D$  are the weights defining the discriminator network.

The process of training a GAN network constitutes a min-max problem such that  $\min_{\theta_G} \max_{\theta_D} V(D, G)$ . The choice of the function  $V(D, G)$  is a vast problem within the field of Computer Science. As demonstrated by [Nowozin et al. \(2016\)](#), any GAN can be interpreted as a special type of variational divergence estimation. Thus, the function  $V(G, D)$  can be placed on the most generic formulation as

$$V(D, G) = \mathbb{E}_{\mathbf{x} \sim p_d(\mathbf{x})} [\mathbb{E}_{y \sim p_d(y)} [g_f(D(y|\mathbf{x}))]] + \mathbb{E}_{\mathbf{z} \sim p_z(\mathbf{z})} [-f^*(g_f(D(G(\mathbf{z}|\mathbf{x}))))], \quad (1)$$

where  $g_f$  denotes the output activation function and  $f^*$  is the corresponding Fenchel conjugate function of  $g_f$  ([Hiriart-Urruty and Lemaréchal, 2001](#)). The functions  $g_f$  and  $f^*$  can be chosen freely, provided they are derived from any  $f$ -divergence ([Csiszár and Shields, 2004](#); [Liese and Vajda, 2006](#); [Nguyen et al., 2007](#); [Reid and Williamson, 2011](#)). Conversely,  $\mathbb{E}_{\mathbf{x} \sim p_d(\mathbf{x})}$ ,  $\mathbb{E}_{y \sim p_d(y)}$  and  $\mathbb{E}_{\mathbf{z} \sim p_d(\mathbf{z})}$  denote the expected values over  $\mathbf{x}$ ,  $y$  and  $\mathbf{z}$  respectively.

Taking this into account, the loss function to be minimized for the discriminator network is given by

$$\mathcal{L}_D(\theta_D) = \frac{-1}{N_{batch}} \sum_{i=1}^{N_{batch}} [g_f(D(y_i|\mathbf{x}_i; \theta_D)) - f^*(g_f(D(G(\mathbf{z}_i|\mathbf{x}_i); \theta_G)|\mathbf{x}_i; \theta_D))], \quad (2)$$

---

<sup>7</sup>Beware that Computer Science standard notation at literature on GANs, name the random vectors with  $z$ . Do not confuse this  $z$  with the redshift of the galaxies (that will be either denoted in this paper as  $y$  or  $\hat{y}$  for spectroscopic or photometric redshifts respectively).

whereas the loss for the generator to be minimized simultaneously is given by

$$\mathcal{L}_G(\theta_G) = \frac{-1}{N_{batch}} \sum_{i=1}^{N_{batch}} g_f(D(G(\mathbf{z}_i|\mathbf{x}_i; \theta_G)|\mathbf{x}_i; \theta_D)). \quad (3)$$

From all the possible  $f$ -divergences, we select the Kullback-Leibler divergence (Kullback and Leibler, 1951), given by

$$D_{KL}(P, Q) = \int P(\mathbf{x}) \ln \left[ \frac{P(\mathbf{x})}{Q(\mathbf{x})} \right] d\mathbf{x}. \quad (4)$$

Thus, by using the KL-divergence as the proposed  $f$ -divergence, the corresponding  $g_f(x)$  and  $g(f^*(x))$  are given by Nowozin et al. (2016)

$$g_f(x) = x \quad (5)$$

and

$$f^*(g_f(x)) = e^{x-1}. \quad (6)$$

By using this  $f$ -divergence approach, the photometric redshift inferred by the generator network -given a fixed set of values for the magnitudes  $\mathbf{x}_i$ , will be a function of the random vector  $\mathbf{z}_j$  such that

$$\hat{y}_i(\mathbf{z}_j) = G(\mathbf{z}_j|\mathbf{x}_i). \quad (7)$$

If  $N_r$  different random vectors are considered, the set of values  $\{\hat{y}_i(\mathbf{z}_j)\}_{j=1}^{N_r}$ , will be a random variable distributed according to the underlying conditional probability density of the spectroscopic redshift for the value of magnitudes  $\mathbf{x}_i$ . Thus, provided that  $N_r$  is large, the distribution of  $\hat{y}_i(\mathbf{z}_j)$  is an estimator of the probability density function of the true spectroscopic redshift for that single  $i$ -th galaxy.

Proposed topology of the neural network for the generator is a sequence of 3 fully connected layers, where the first two layers are followed by a Batch Normalization layer and a ReLU activation function. Input neurons of the first fully connected layer has  $4 + Z_{DIM}$  neurons with  $G_{DIM}$  output neurons. Hidden fully connected layer consist of  $G_{DIM}$  input neurons and  $G_{DIM}$  output neurons. Final fully connected layer consist of  $G_{DIM}$  input neurons and a single output neuron. The input of the generator network is composed by the vector  $\mathbf{x}$  of the four galaxy magnitudes and the random vector  $\mathbf{z}$ . The

output of the generator network is directly the inferred photometric redshift  $\hat{y}$ .

For the discriminator neural network a sequence of 3 fully connected layers, where the first two layers are followed by a Batch Normalization layer and a ReLU activation function. Input neurons of the first fully connected layer has 5 neurons with  $D_{DIM}$  output neurons. Hidden fully connected layer consist of  $D_{DIM}$  input neurons and  $D_{DIM}$  output neurons. Final fully connected layer consist of  $D_{DIM}$  input neurons and a single output neuron followed by a sigmoid activation function,  $\sigma(x) = 1/(1 + e^{-x})$ . The input of the discriminator network is composed by a redshift (spectroscopic  $-y$ - or photometric  $-\hat{y}$ -), and the vector  $\mathbf{x}$  of galaxy magnitudes. The output of the discriminator network is a decimal number between 0 and 1 that indicates the probability of the input galaxy to be real.

Topology of generator and discriminator neural networks can be seen at [Figure 1](#).

In order to compare the results of the proposed CGAN with classic machine-learning approaches, a Random Forest regressor is also employed ([Breiman, 2001](#))

### 3. Data Analysis

Proposed CGAN was tested at DES-Y1 data spectroscopy-matched with SDSS galaxies. Data was taken from the public data releases DR1 ([Abbott et al., 2018](#); [Drlica-Wagner et al., 2018](#)) from The Dark Energy Survey Collaboration that are available at the NCSA repository<sup>8</sup>.

Code for the CGAN was implemented under Python<sup>9</sup> using PyTorch<sup>10</sup> ([Paszke et al., 2019](#)), whereas code for the Random Forest Regressor was implemented using Scikit-Learn<sup>11</sup> ([Pedregosa et al., 2011](#)). Full code of this analysis can be found at author’s GitHub repository<sup>12</sup>.

From the DES-Y1 proposed sample, we take the Stripe-82 subset of galaxies with matched spectroscopic redshift from SDSS. For consideration of the sample, we restrict ourselves to the galaxies with spectroscopic redshift

---

<sup>8</sup><https://des.ncsa.illinois.edu/releases/y1a1>

<sup>9</sup><https://www.python.org>

<sup>10</sup><https://pytorch.org>

<sup>11</sup><https://scikit-learn.org>

<sup>12</sup><https://github.com/mgarciafernandez-uem/CGAN-photoz>

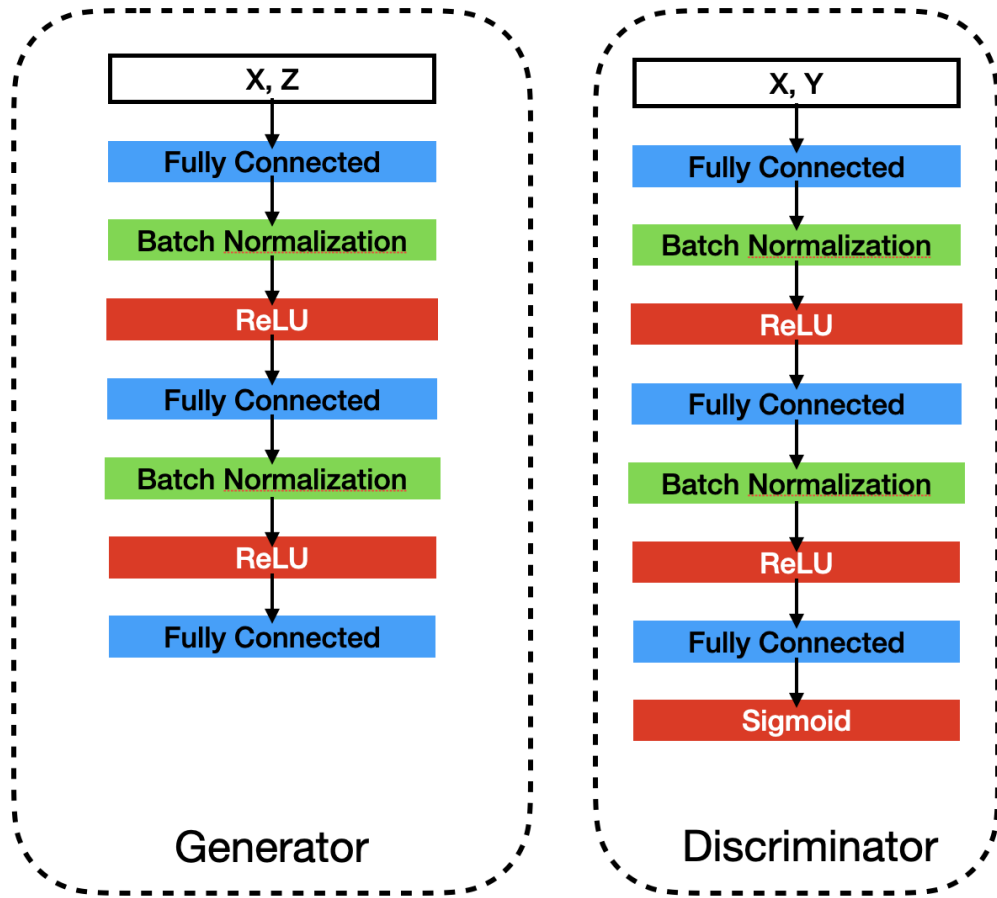


Figure 1: Topology of the neural networks used. Blue boxes denote the fully connected layers, green boxes denote the normalization layers and red boxes denote the activation functions.

Hyperparameter	Value
$Z_{DIM}$	20
$D_{DIM}$	32
$G_{DIM}$	32

Table 1: Hyperparameters of the CGAN used for this paper.

$0.0 < z_{sp} < 0.8$ . This quality cut is imposed to avoid a very long tail up to redshift 2, but with a few galaxies, as the inclusion of these elements on the training sample of the algorithm can potentially introduce biases due to the neural network infer magnitude-redshift relationships from an under-represented sample of galaxies of high-redshift. Selected measurements of magnitudes for the galaxies are the `MAG_AUTO` magnitudes at the *griz* band-pass filters as measured by `SExtractor` (Bertin and Arnouts, 1996). The distribution of the *griz* magnitudes and spectroscopic redshift of the selected calibration sample of galaxies can be seen along with their correlation plots at Figure 2. Total number of galaxies at the final calibration sample is 33410. From this final calibration sample, we do a split between a training sample and a test sample with 80% and 20% of the galaxies respectively. The training sample is used for determining the parameters of the photometric redshift algorithm during the training process. On the other side, the test sample is used for measuring the properties of the algorithm on a set of galaxies unseen by the photometric redshift algorithm.

Hyperparameters of the model defining the sizes of the dense layers of generator ( $G_{DIM}$ ) and the discriminator ( $D_{DIM}$ ) along with the size the random vector ( $Z_{DIM}$ ) can be seen at Table 1. Training strategy used the Adam optimizer with a learning rate parameter of  $lr = 10^{-4}$  for both generator and discriminator network using 10000 training epochs, using a step learning-rate approach reducing the learning rate by a factor of 0.2 every 2000 training epochs. Training strategy is the same for the generator and the discriminator networks. The loss for both generator and discriminator as a function of the training epoch can be seen at Figure 3, showing a good and stable convergence of the losses for both the generator and discriminator networks.

A comparison of the observed distribution of inferred redshift of galaxies for the test sample is compared with the true spectroscopic redshift can be seen at Figure 4. In addition, a comparison of the dispersion between the true spectroscopic redshift and the inferred photometric redshift can be see at



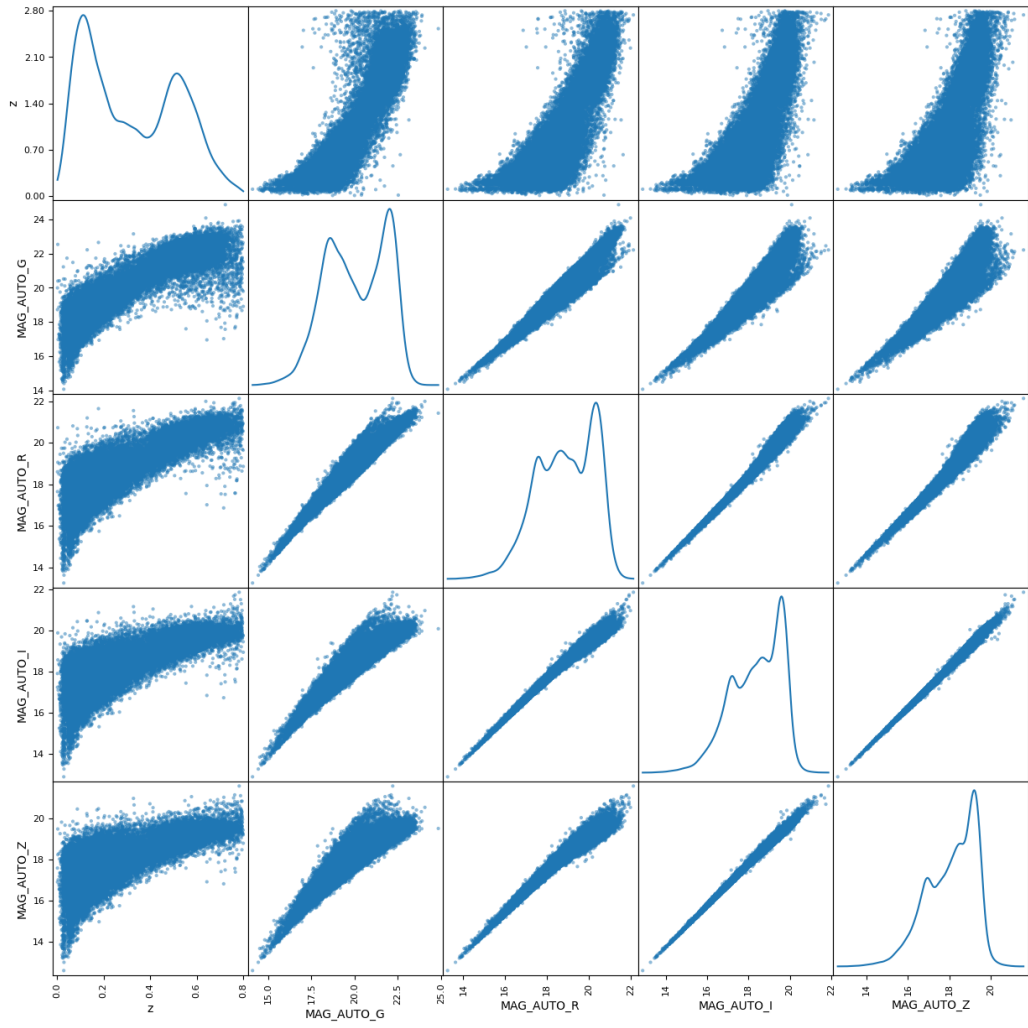


Figure 2: Distribution and correlation of the *griz* MAG\_AUTO magnitudes and the measured spectroscopic redshift

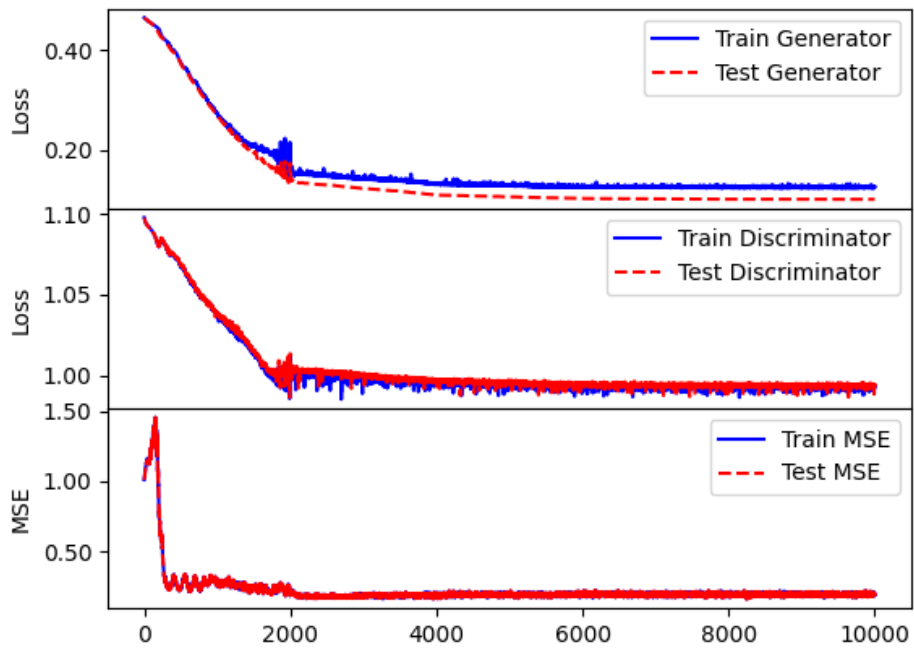


Figure 3: Loss function for the generator and discriminator networks as a function of the training epoch as measured at the training and test data samples. Values of the measured losses have been shifted +1 in order to avoid negative values at the Y-axis. A plot showing the Mean Square Error (MSE) between the inferred photometric redshift and the true spectroscopic redshift is also displayed.

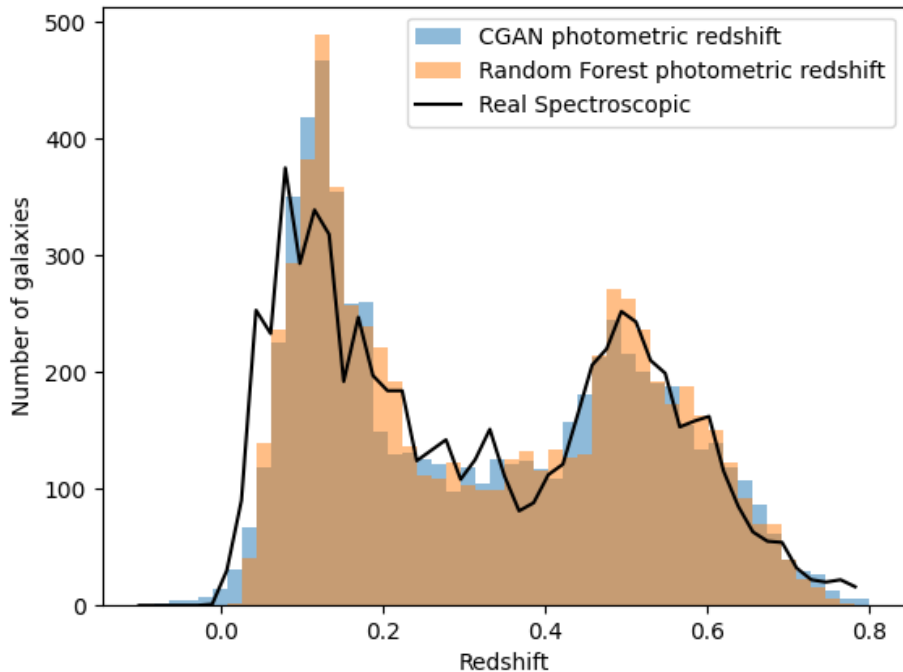


Figure 4: Distribution of the photometric redshift of galaxies inferred from both proposed CGAN approach and the classic Random Forest algorithm. Both distributions are compared with the true spectroscopic redshift (black solid-line). Measurements are made on the test sample of galaxies.

Figure 5. From these plots, we can see that the photometric redshifts inferred by the proposed CGAN approach can accurately trace the true spectroscopic redshift distribution of the test sample of galaxies, reaching an agreement similar to the classic Random Forest Regressor. In addition, we can see that there is a similar level of dispersion on the photometric redshifts inferred by the CGAN approach and the Random Forest Regressor. It is important to remark that no significant biases or asymmetries are spotted. We see that dispersion of inferred photometric redshift randomly fluctuate around the true spectroscopic redshift for all the range of values of redshift.

Quality metrics for photometric redshift determination are based on the ones proposed at Sánchez et al. (2014) and can be found at Table 2. Used quality metrics for photometric comparison, are: the mean bias between

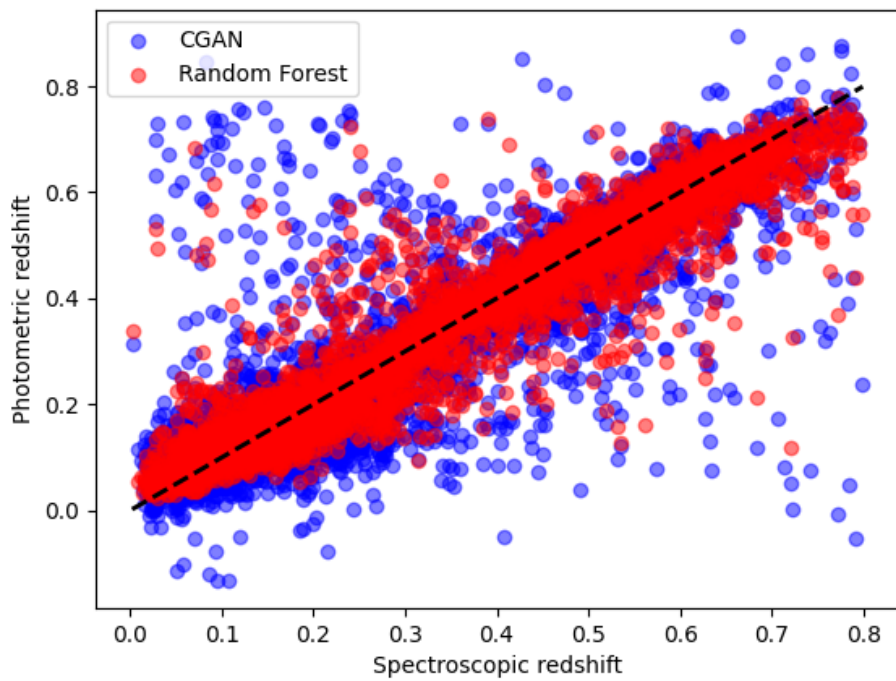


Figure 5: Dispersion between the photometric redshift inferred by proposed CGAN and classic Random Forest algorithm and the true spectroscopic redshift. The black-dashed line displays those redshifts where the photometric redshift is equal to the spectroscopic redshift. Measurements are made on the test sample of galaxies.

Parameter	Description	CGAN	Random Forest
$\Delta z$	Mean bias	-0.0046	-0.0030
$\Delta z_{50}$	Median of the bias	-0.0046	-0.0055
$\sigma_{\Delta z}$	Standard deviation of the bias	0.092	0.056
$out_{2\sigma}$	Outliers beyond 2 standard deviations	4%	5%
$out_{3\sigma}$	Outliers beyond 3 standard deviations	2%	2%

Table 2: Quality measures for the photometric redshift determination as measured on the test sample.

the photometric redshift and the spectroscopic redshift ( $\bar{\Delta z}$ ), the median of the bias ( $\Delta z_{50}$ ), the standard deviation of the bias ( $\sigma_{\Delta z}$ ), the fraction of galaxies with spectroscopic redshift outside of the two-standard deviation range ( $out_{2\sigma}$ ) and the fraction of galaxies with spectroscopic redshift outside of the three-standard deviation range ( $out_{3\sigma}$ ).

Both CGAN and Random Forest Regressor show a similar level of performance. As a comparison with other quality tests from other photometric redshift algorithms made with DES data, we see that the fraction of outliers of the proposed CGAN is at a comparable level with the 15 photometric redshift algorithms proposed at Table 8 from [Sánchez et al. \(2014\)](#). Nevertheless, our proposed CGAN has one order of magnitude better precision for the mean and median bias, reaching only 3 out of the 15 algorithms a comparable magnitude to the one obtained by the proposed CGAN of this paper: TPZ, SkyNet and ANNz.

As an additional by-product, we can inspect the redshift probability density inferred by the CGAN for individual galaxies. At [Figure 6](#), we can see 9 randomly selected galaxies, comparing the inferred probability density function with the respective true spectroscopic redshift. Testing if the probability densities of the redshift inferred for individual galaxies can not be directly sampling the spectroscopic redshift, as we only have one single galaxy. Nevertheless, we can make use of the Chebyshev inequality to probe that the photometric redshift produced by our CGAN is indeed a probability distribution. Chebyshev inequality states that if  $P$  is any probability density with mean photometric redshift  $\mu$  and variance  $\sigma$ , then,  $\forall a > 0$  the following inequality holds ([Canavos et al., 1988](#)),

$$P(|\hat{y} - \mu| \geq a\sigma) \leq \frac{1}{a^2}. \quad (8)$$

Thus, for each individual galaxy, its photometric redshift for the probabil-

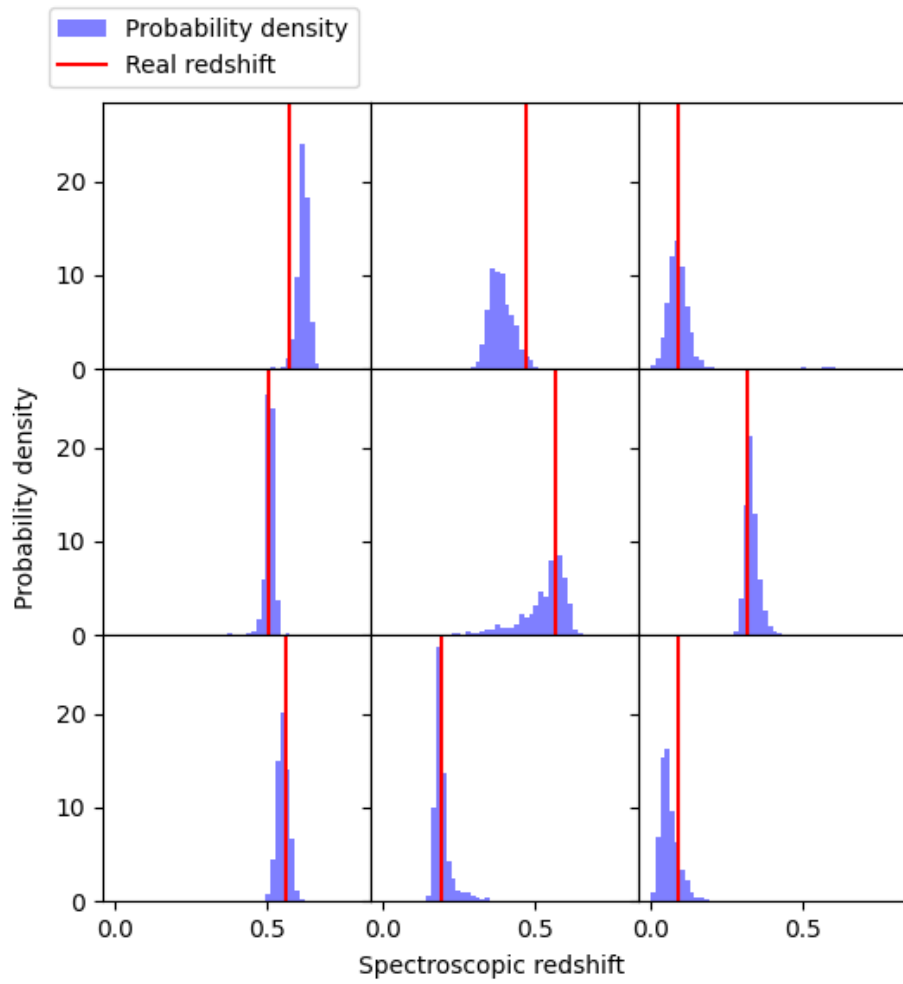


Figure 6: Probability densities generated by the CGAN proposed on this paper compared with the true spectroscopic redshift measured at the test sample.

ity density is generated. From this probability density, the mean and the standard deviation is computed. Nine different values of  $a$  are considered beforehand and the number of galaxies for which the inequality  $|\hat{y} - \mu| \geq a\sigma$  holds is computed. By Chebyshev inequality, the fraction of outliers for every  $a$  shall be lower or equal to  $1/a^2$ .

At [Figure 7](#), we can see the fraction of outliers measured by the CGAN compared with the upper bound imposed by the Chebyshev inequality. We can see that the fraction of outliers is below the Chebyshev bound for all values of  $a$ . Thus, we can conclude that the photometric redshift probability densities inferred by the CGAN, are indeed a probability density. Nevertheless, we can not demonstrate how accurate these probability densities represent the real spectroscopic redshift for individual galaxies.

#### 4. Conclusions

On this paper, it was presented a new machine-learning technique for photometric redshift estimation using Conditional Generative Adversarial Networks (CGANs), was presented. Proposed CGAN technique was tested using Dark Energy Survey Y1 data and compared with the classic machine-learning technique the Random Forest Regressor.

Results obtained at CGAN approach, exhibit a similar performance for determining the mean photometric redshift as the Random Forest Classifier. Whereas Random Forest Regressor can only provide a the expected redshift for each individual galaxy, the proposed CGAN approach is able to provide a full probability density function. This additional capability of the CGAN, allows for a better control for the impact of thick tails of the distribution, making this type of photometric redshift algorithmic approach more suitable for cosmological probes that are specially sensitive to thick tails at photometric redshifts -such as number-counts magnification-.

In addition to the value added, CGAN demonstrates a superior computing performance over Random Forest Regressor, as modern Deep Learning frameworks -such as PyTorch-, have a strong parallelization optimization for the determination of the weights of the tensors defining the neural networks, whereas algorithms such as the Random Forest Regressor are not parallelization. This, makes the CGAN approach superior from the computing performance point of view, which is specially suitable for large Cosmology surveys.

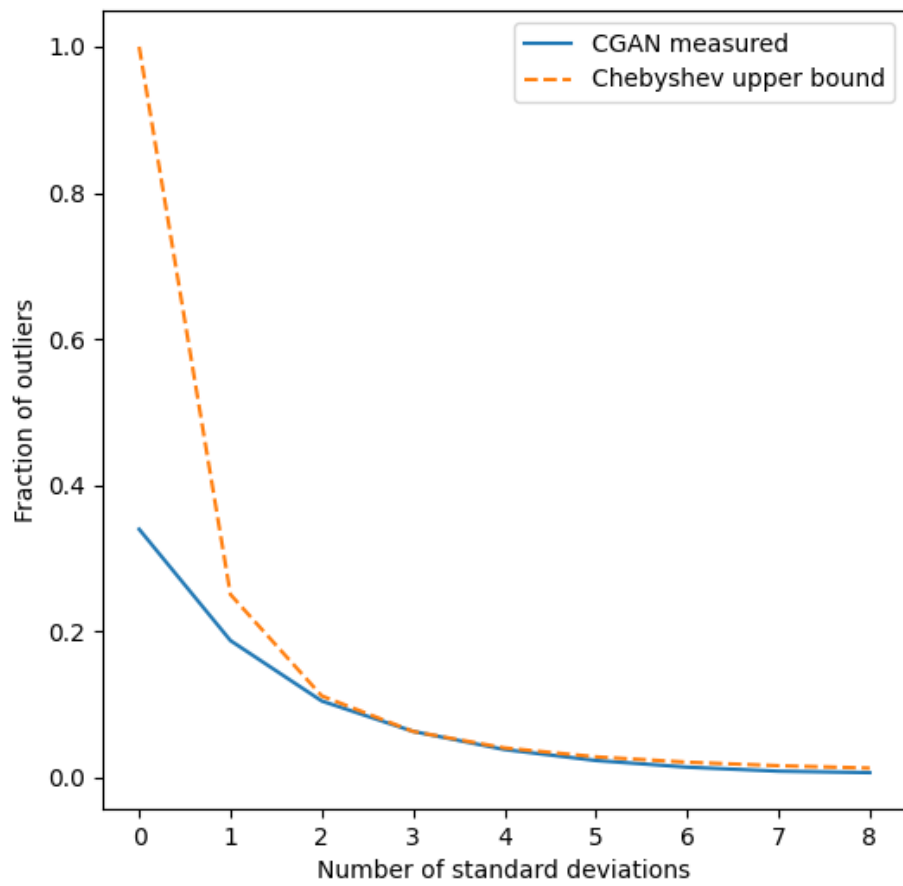


Figure 7: Validation of the Chebyshev inequality for the test data sample.



It is worth remarking that the results of this work do not constitute a full out-of-the-box software for photometric redshift determination, rather than a proof of concept and a feasibility analysis. This algorithm has still room for improvement in terms of calibration sample selection and the inclusion of additional features.

Accuracy metrics obtained by CGAN, exhibit a performance ranking with the best photometric redshift trained on similar calibration data. Performance and accuracy metrics obtained by the CGAN approach described here, is strongly limited by the resolution of the band-pass filters used for the photometry and the galaxy sample used. On this dataset, only four band-pass filters *griz* are available, thus, much better photometric redshift could be obtained by using a higher resolution apparatus, like the 40-band-pass filter PAUCam.

Future work will explore the possibility of including a finer selection by population of galaxies (main-sequence, LRGs, etc.) that can be included as an additional parameter of the CGAN. Additional features to be explored will also include an evaluation of the inclusion of additional photometric features of the galaxies, such as shape parameters.

## Acknowledgements

Author wants to thank to Departamento de Computación y Tecnología of Universidad Europea de Madrid for providing access to computing resources at the LORCA Cluster.

## References

Abbott, T.M.C., Abdalla, F.B., Allam, S., Amara, A., Annis, J., Asorey, J., Avila, S., Ballester, O., Banerji, M., Barkhouse, W., Baruah, L., Baumer, M., Bechtol, K., Becker, M.R., Benoit-Lévy, A., Bernstein, G.M., Bertin, E., Blazek, J., Bocquet, S., Brooks, D., Brout, D., Buckley-Geer, E., Burke, D.L., Busti, V., Campisano, R., Cardiel-Sas, L., Carnero Rosell, A., Carrasco Kind, M., Carretero, J., Castander, F.J., Cawthon, R., Chang, C., Chen, X., Conselice, C., Costa, G., Croce, M., Cunha, C.E., D’Andrea, C.B., da Costa, L.N., Das, R., Daues, G., Davis, T.M., Davis, C., De Vicente, J., DePoy, D.L., DeRose, J., Desai, S., Diehl, H.T., Dietrich, J.P., Dodelson, S., Doel, P., Drlica-Wagner, A., Eifler, T.F., Elliott, A.E., Evrard, A.E., Farahi, A., Fausti Neto, A., Fernandez, E., Finley, D.A.,

Flaugher, B., Foley, R.J., Fosalba, P., Friedel, D.N., Frieman, J., García-Bellido, J., Gaztanaga, E., Gerdes, D.W., Giannantonio, T., Gill, M.S.S., Glazebrook, K., Goldstein, D.A., Gower, M., Gruen, D., Gruendl, R.A., Gschwend, J., Gupta, R.R., Gutierrez, G., Hamilton, S., Hartley, W.G., Hinton, S.R., Hislop, J.M., Hollowood, D., Honscheid, K., Hoyle, B., Huterer, D., Jain, B., James, D.J., Jeltema, T., Johnson, M.W.G., Johnson, M.D., Kacprzak, T., Kent, S., Khullar, G., Klein, M., Kovacs, A., Koziol, A.M.G., Krause, E., Kremin, A., Kron, R., Kuehn, K., Kuhlmann, S., Kuropatkin, N., Lahav, O., Lasker, J., Li, T.S., Li, R.T., Liddle, A.R., Lima, M., Lin, H., López-Reyes, P., MacCrann, N., Maia, M.A.G., Maloney, J.D., Manera, M., March, M., Marriner, J., Marshall, J.L., Martini, P., McClintock, T., McKay, T., McMahon, R.G., Melchior, P., Menanteau, F., Miller, C.J., Miquel, R., Mohr, J.J., Morganson, E., Mould, J., Neilsen, E., Nichol, R.C., Nogueira, F., Nord, B., Nugent, P., Nunes, L., Ogando, R.L.C., Old, L., Pace, A.B., Palmese, A., Paz-Chinchón, F., Peiris, H.V., Percival, W.J., Petravick, D., Plazas, A.A., Poh, J., Pond, C., Porredon, A., Pujol, A., Refregier, A., Reil, K., Ricker, P.M., Rollins, R.P., Romer, A.K., Roodman, A., Rooney, P., Ross, A.J., Rykoff, E.S., Sako, M., Sanchez, M.L., Sanchez, E., Santiago, B., Saro, A., Scarpine, V., Scolnic, D., Serrano, S., Sevilla-Noarbe, I., Sheldon, E., Shipp, N., Silveira, M.L., Smith, M., Smith, R.C., Smith, J.A., Soares-Santos, M., Sobreira, F., Song, J., Stebbins, A., Suchyta, E., Sullivan, M., Swanson, M.E.C., Tarle, G., Thaler, J., Thomas, D., Thomas, R.C., Troxel, M.A., Tucker, D.L., Vikram, V., Vivas, A.K., Walker, A.R., Wechsler, R.H., Weller, J., Wester, W., Wolf, R.C., Wu, H., Yanny, B., Zenteno, A., Zhang, Y., Zuntz, J., DES Collaboration, Juneau, S., Fitzpatrick, M., Nikutta, R., 2018. The Dark Energy Survey: Data Release 1. *Astrophysical Journal, Supplement* 239, 18. doi:[10.3847/1538-4365/aae9f0](https://doi.org/10.3847/1538-4365/aae9f0), [arXiv:1801.03181](https://arxiv.org/abs/1801.03181).

Almosallam, I.A., Jarvis, M.J., Roberts, S.J., 2016. GPZ: non-stationary sparse Gaussian processes for heteroscedastic uncertainty estimation in photometric redshifts. *Monthly Notices of the Royal Astronomical Society* 462, 726–739. doi:[10.1093/mnras/stw1618](https://doi.org/10.1093/mnras/stw1618), [arXiv:1604.03593](https://arxiv.org/abs/1604.03593).

Arnouts, S., Ilbert, O., 2011. LePHARE: Photometric Analysis for Redshift Estimate. *Astrophysics Source Code Library*, record ascl:1108.009.

Benítez, N., 2011. BPZ: Bayesian Photometric Redshift Code. *Astrophysics Source Code Library*, record ascl:1108.011.

- Bertin, E., Arnouts, S., 1996. SExtractor: Software for source extraction. *Astronomy and Astrophysics, Supplement* 117, 393–404. doi:[10.1051/aas:1996164](https://doi.org/10.1051/aas:1996164).
- Bishop, C.M., 2006. *Pattern Recognition and Machine Learning*. Information Science and Statistics, Springer.
- Bolzonella, M., Miralles, J.M., Pelló, R., 2011. Hyperz: Photometric Redshift Code. *Astrophysics Source Code Library*, record ascl:1108.010.
- Breiman, L., 2001. Random forests. *Machine Learning* 45, 5–32. URL: <https://doi.org/10.1023/A:1010933404324>, doi:[10.1023/A:1010933404324](https://doi.org/10.1023/A:1010933404324).
- Canavos, G.C., Urbina Medal, E.G., Valencia Ramírez, G.J., 1988. *Probabilidad y estadística : aplicaciones y métodos*. McGraw-Hill/ Interamericana de México, México [etc.
- Carrasco Kind, M., Brunner, R.J., 2013. TPZ: photometric redshift PDFs and ancillary information by using prediction trees and random forests. *Monthly Notices of the Royal Astronomical Society* 432, 1483–1501. doi:[10.1093/mnras/stt574](https://doi.org/10.1093/mnras/stt574), [arXiv:1303.7269](https://arxiv.org/abs/1303.7269).
- Cavuoti, S., Amaro, V., Brescia, M., Vellucci, C., Tortora, C., Longo, G., 2017. METAPHOR: a machine-learning-based method for the probability density estimation of photometric redshifts. *Monthly Notices of the Royal Astronomical Society* 465, 1959–1973. doi:[10.1093/mnras/stw2930](https://doi.org/10.1093/mnras/stw2930), [arXiv:1611.02162](https://arxiv.org/abs/1611.02162).
- Chang, C.C., Lin, C.J., 2011. Libsvm: A library for support vector machines. *ACM Trans. Intell. Syst. Technol.* 2. URL: <https://doi.org/10.1145/1961189.1961199>, doi:[10.1145/1961189.1961199](https://doi.org/10.1145/1961189.1961199).
- Chunduri, K., Mahesh, M., 2023. Deep Learning Approach to Photometric Redshift Estimation. *arXiv e-prints* , [arXiv:2310.16304](https://arxiv.org/abs/2310.16304)doi:[10.48550/arXiv.2310.16304](https://doi.org/10.48550/arXiv.2310.16304), [arXiv:2310.16304](https://arxiv.org/abs/2310.16304).
- Collister, A.A., Lahav, O., 2004. ANNz: Estimating Photometric Redshifts Using Artificial Neural Networks. *Publications of the ASP* 116, 345–351. doi:[10.1086/383254](https://doi.org/10.1086/383254), [arXiv:astro-ph/0311058](https://arxiv.org/abs/astro-ph/0311058).

- Crocce, M., Ross, A.J., Sevilla-Noarbe, I., Gaztanaga, E., Elvin-Poole, J., Avila, S., Alarcon, A., Chan, K.C., Banik, N., Carretero, J., Sanchez, E., Hartley, W.G., Sánchez, C., Giannantonio, T., Rosenfeld, R., Salvador, A.I., Garcia-Fernandez, M., García-Bellido, J., Abbott, T.M.C., Abdalla, F.B., Allam, S., Annis, J., Bechtol, K., Benoit-Lévy, A., Bernstein, G.M., Bernstein, R.A., Bertin, E., Brooks, D., Buckley-Geer, E., Rosell, A.C., Kind, M.C., Castander, F.J., Cawthon, R., Cunha, C.E., D'Andrea, C.B., da Costa, L.N., Davis, C., De Vicente, J., Desai, S., Diehl, H.T., Doel, P., Drlica-Wagner, A., Eifler, T.F., Fosalba, P., Frieman, J., García-Bellido, J., Gerdes, D.W., Gruen, D., Gruendl, R.A., Gschwend, J., Gutierrez, G., Hollowood, D., Honscheid, K., Jain, B., James, D.J., Krause, E., Kuehn, K., Kuhlmann, S., Kuropatkin, N., Lahav, O., Lima, M., Maia, M.A.G., Marshall, J.L., Martini, P., Menanteau, F., Miller, C.J., Miquel, R., Nichol, R.C., Percival, W.J., Plazas, A.A., Sako, M., Scarpine, V., Schindler, R., Scolnic, D., Sheldon, E., Smith, M., Smith, R.C., Soares-Santos, M., Sobreira, F., Suchyta, E., Swanson, M.E.C., Tarle, G., Thomas, D., Tucker, D.L., Vikram, V., Walker, A.R., Yanny, B., Zhang, Y., Collaboration, D.E.S., 2018. Dark energy survey year 1 results: galaxy sample for bao measurement. *Monthly Notices of the Royal Astronomical Society* 482, 2807–2822. URL: <https://doi.org/10.1093/mnras/sty2522>, doi:10.1093/mnras/sty2522, arXiv:<https://academic.oup.com/mnras/article-pdf/482/2/2807/26576969/sty2522.pdf>
- Csiszár, I., Shields, P., 2004. Information theory and statistics: A tutorial. *Foundations and Trends® in Communications and Information Theory* 1, 417–528. URL: <http://dx.doi.org/10.1561/0100000004>, doi:10.1561/0100000004.
- D'Isanto, A., Polsterer, K.L., 2018. Photometric redshift estimation via deep learning. Generalized and pre-classification-less, image based, fully probabilistic redshifts. *Astronomy and Astrophysics* 609, A111. doi:10.1051/0004-6361/201731326, arXiv:1706.02467.
- Drlica-Wagner, A., Sevilla-Noarbe, I., Rykoff, E.S., Gruendl, R.A., Yanny, B., Tucker, D.L., Hoyle, B., Rosell, A.C., Bernstein, G.M., Bechtol, K., Becker, M.R., Benoit-Lévy, A., Bertin, E., Kind, M.C., Davis, C., de Vicente, J., Diehl, H.T., Gruen, D., Hartley, W.G., Leistedt, B., Li, T.S., Marshall, J.L., Neilsen, E., Rau, M.M., Sheldon, E., Smith, J., Troxel, M.A., Wyatt, S., Zhang, Y., Abbott, T.M.C., Abdalla, F.B., Allam, S.,

Banerji, M., Brooks, D., Buckley-Geer, E., Burke, D.L., Capozzi, D., Carretero, J., Cunha, C.E., D’Andrea, C.B., da Costa, L.N., DePoy, D.L., Desai, S., Dietrich, J.P., Doel, P., Evrard, A.E., Neto, A.F., Flaughner, B., Fosalba, P., Frieman, J., García-Bellido, J., Gerdes, D.W., Giannantonio, T., Gschwend, J., Gutierrez, G., Honscheid, K., James, D.J., Jeltama, T., Kuehn, K., Kuhlmann, S., Kuropatkin, N., Lahav, O., Lima, M., Lin, H., Maia, M.A.G., Martini, P., McMahon, R.G., Melchior, P., Menanteau, F., Miquel, R., Nichol, R.C., Ogando, R.L.C., Plazas, A.A., Romer, A.K., Roodman, A., Sanchez, E., Scarpine, V., Schindler, R., Schubnell, M., Smith, M., Smith, R.C., Soares-Santos, M., Sobreira, F., Suchyta, E., Tarle, G., Vikram, V., Walker, A.R., Wechsler, R.H., Zuntz, J., Collaboration), D., 2018. Dark energy survey year 1 results: The photometric data set for cosmology. *The Astrophysical Journal Supplement Series* 235, 33. URL: <https://dx.doi.org/10.3847/1538-4365/aab4f5>, doi:10.3847/1538-4365/aab4f5.

Garcia-Fernandez, M., Sanchez, E., Sevilla-Noarbe, I., Suchyta, E., Huff, E.M., Gaztanaga, E., Aleksić, J., Ponce, R., Castander, F.J., Hoyle, B., Abbott, T.M.C., Abdalla, F.B., Allam, S., Annis, J., Benoit-Lévy, A., Bernstein, G.M., Bertin, E., Brooks, D., Buckley-Geer, E., Burke, D.L., Carnero Rosell, A., Carrasco Kind, M., Carretero, J., Crocce, M., Cunha, C.E., D’Andrea, C.B., da Costa, L.N., DePoy, D.L., Desai, S., Diehl, H.T., Eifler, T.F., Evrard, A.E., Fernandez, E., Flaughner, B., Fosalba, P., Frieman, J., García-Bellido, J., Gerdes, D.W., Giannantonio, T., Gruen, D., Gruendl, R.A., Gschwend, J., Gutierrez, G., James, D.J., Jarvis, M., Kirk, D., Krause, E., Kuehn, K., Kuropatkin, N., Lahav, O., Lima, M., MacCrann, N., Maia, M.A.G., March, M., Marshall, J.L., Melchior, P., Miquel, R., Mohr, J.J., Plazas, A.A., Romer, A.K., Roodman, A., Rykoff, E.S., Scarpine, V., Schubnell, M., Smith, R.C., Soares-Santos, M., Sobreira, F., Tarle, G., Thomas, D., Walker, A.R., Wester, W., Collaboration), T.D., 2018. Weak lensing magnification in the dark energy survey science verification data. *Monthly Notices of the Royal Astronomical Society* 476, 1071–1085. URL: <https://doi.org/10.1093/mnras/sty282>, doi:10.1093/mnras/sty282, arXiv:<https://academic.oup.com/mnras/article-pdf/476/1/1071/24239965/sty282.pdf>.

Gerdes, D.W., Sypniewski, A.J., McKay, T.A., Hao, J., Weis, M.R., Wechsler, R.H., Busha, M.T., 2010. *ArborZ: Photometric Redshifts Using*

- Boosted Decision Trees. *Astrophysical Journal* 715, 823–832. doi:[10.1088/0004-637X/715/2/823](https://doi.org/10.1088/0004-637X/715/2/823), [arXiv:0908.4085](https://arxiv.org/abs/0908.4085).
- Goodfellow, I., Bengio, Y., Courville, A., 2016. *Deep Learning*. MIT Press. <http://www.deeplearningbook.org>.
- Goodfellow, I.J., Pouget-Abadie, J., Mirza, M., Xu, B., Warde-Farley, D., Ozair, S., Courville, A., Bengio, Y., 2014. Generative adversarial nets, in: *Proceedings of the 27th International Conference on Neural Information Processing Systems - Volume 2*, MIT Press, Cambridge, MA, USA. p. 2672–2680.
- Graham, M.L., Connolly, A.J., Ivezić, Ž., Schmidt, S.J., Jones, R.L., Jurić, M., Daniel, S.F., Yoachim, P., 2018. Photometric Redshifts with the LSST: Evaluating Survey Observing Strategies. *Astronomical Journal* 155, 1. doi:[10.3847/1538-3881/aa99d4](https://doi.org/10.3847/1538-3881/aa99d4), [arXiv:1706.09507](https://arxiv.org/abs/1706.09507).
- Hiriart-Urruty, J.B., Lemaréchal, C., 2001. *Fundamentals of Convex Analysis* / J.B. Hiriart-Urruty, C. Lemaréchal. doi:[10.1007/978-3-642-56468-0](https://doi.org/10.1007/978-3-642-56468-0).
- Hoyle, B., 2016. Measuring photometric redshifts using galaxy images and deep neural networks. *Astronomy and Computing* 16, 34–40. URL: <https://www.sciencedirect.com/science/article/pii/S221313371630021X>, doi:<https://doi.org/10.1016/j.ascom.2016.03.006>.
- Kullback, S., Leibler, R.A., 1951. On Information and Sufficiency. *The Annals of Mathematical Statistics* 22, 79 – 86. URL: <https://doi.org/10.1214/aoms/1177729694>, doi:[10.1214/aoms/1177729694](https://doi.org/10.1214/aoms/1177729694).
- Laur, J., Tempel, E., Tamm, A., Kipper, R., Liivamägi, L.J., Hernán-Caballero, A., Muru, M.M., Chaves-Montero, J., Díaz-García, L.A., Turner, S., Tuvikene, T., Queiroz, C., Bom, C.R., Fernández-Ontiveros, J.A., González Delgado, R.M., Civera, T., Abramo, R., Alcaniz, J., Benítez, N., Bonoli, S., Carneiro, S., Cenarro, J., Cristóbal-Hornillos, D., Dupke, R., Ederoclite, A., López-Sanjuan, C., Marín-Franch, A., de Oliveira, C.M., Moles, M., Sodr e, L., Taylor, K., Varela, J., Vázquez Ramió, H., 2022. TOPz: Photometric redshifts for J-PAS. *Astronomy and Astrophysics* 668, A8. doi:[10.1051/0004-6361/202243881](https://doi.org/10.1051/0004-6361/202243881), [arXiv:2209.01040](https://arxiv.org/abs/2209.01040).

- Liese, F., Vajda, I., 2006. On divergences and informations in statistics and information theory. *IEEE Transactions on Information Theory* 52, 4394–4412. doi:[10.1109/TIT.2006.881731](https://doi.org/10.1109/TIT.2006.881731).
- Lima, E., Sodré, L., Bom, C., Teixeira, G., Nakazono, L., Buzzo, M., Queiroz, C., Herpich, F., Castellon, J.N., Dantas, M., Dors, O., de Souza, R.T., Akras, S., Jiménez-Teja, Y., Kanaan, A., Ribeiro, T., Schoennell, W., 2022. Photometric redshifts for the s-plus survey: Is machine learning up to the task? *Astronomy and Computing* 38, 100510. URL: <https://www.sciencedirect.com/science/article/pii/S2213133721000640>, doi:<https://doi.org/10.1016/j.ascom.2021.100510>.
- Lu, J., Luo, Z., Chen, Z., Fu, L., Du, W., Gong, Y., Li, Y., Meng, X.M., Tang, Z., Zhang, S., Shu, C., Zhou, X., Fan, Z., 2023. Estimating photometric redshift from mock flux for csst survey by using weighted random forest. *Monthly Notices of the Royal Astronomical Society* 527, 12140–12153. URL: <https://doi.org/10.1093/mnras/stad3976>, doi:[10.1093/mnras/stad3976](https://doi.org/10.1093/mnras/stad3976), arXiv:<https://academic.oup.com/mnras/article-pdf/527/4/12140/55462380/stad3976.pdf>.
- Luo, Z., Li, Y., Lu, J., Chen, Z., Fu, L., Zhang, S., Xiao, H., Du, W., Gong, Y., Shu, C., Ma, W., Meng, X., Zhou, X., Fan, Z., 2024. Photometric redshift estimation for CSST survey with LSTM neural networks. *Monthly Notices of the Royal Astronomical Society* 535, 1844–1855. doi:[10.1093/mnras/stae2446](https://doi.org/10.1093/mnras/stae2446), arXiv:[2410.19402](https://arxiv.org/abs/2410.19402).
- Mahmud Pathi, I., Soo, J.Y.H., Jie Wee, M., Nadhilah Zakaria, S., Azwin Ismail, N., Baugh, C.M., Manzoni, G., Gaztanaga, E., Castander, F.J., Eriksen, M., Carretero, J., Fernandez, E., Garcia-Bellido, J., Miquel, R., Padilla, C., Renard, P., Sanchez, E., Sevilla-Noarbe, I., Tallada-Crespí, P., 2024. ANNZ+: an enhanced photometric redshift estimation algorithm with applications on the PAU Survey. arXiv e-prints , arXiv:2409.09981doi:[10.48550/arXiv.2409.09981](https://doi.org/10.48550/arXiv.2409.09981), arXiv:2409.09981.
- Mirza, M., Osindero, S., 2014. Conditional Generative Adversarial Nets. arXiv e-prints , arXiv:1411.1784doi:[10.48550/arXiv.1411.1784](https://doi.org/10.48550/arXiv.1411.1784), arXiv:1411.1784.

- Newman, J.A., Gruen, D., 2022. Photometric Redshifts for Next-Generation Surveys. *Annual Review of Astronomy and Astrophysics* 60, 363–414. doi:[10.1146/annurev-astro-032122-014611](https://doi.org/10.1146/annurev-astro-032122-014611), [arXiv:2206.13633](https://arxiv.org/abs/2206.13633).
- Nguyen, X., Wainwright, M.J., Jordan, M., 2007. Estimating divergence functionals and the likelihood ratio by penalized convex risk minimization, in: Platt, J., Koller, D., Singer, Y., Roweis, S. (Eds.), *Advances in Neural Information Processing Systems*, Curran Associates, Inc. URL: [https://proceedings.neurips.cc/paper\\_files/paper/2007/file/72da7fd6d1302c0a159f6436d01e9eb0-Paper.pdf](https://proceedings.neurips.cc/paper_files/paper/2007/file/72da7fd6d1302c0a159f6436d01e9eb0-Paper.pdf).
- Nowozin, S., Cseke, B., Tomioka, R., 2016. f-gan: Training generative neural samplers using variational divergence minimization, in: Lee, D., Sugiyama, M., Luxburg, U., Guyon, I., Garnett, R. (Eds.), *Advances in Neural Information Processing Systems*, Curran Associates, Inc. URL: [https://proceedings.neurips.cc/paper\\_files/paper/2016/file/cedebb6e872f539bef8c3f919874e9d7-Paper.pdf](https://proceedings.neurips.cc/paper_files/paper/2016/file/cedebb6e872f539bef8c3f919874e9d7-Paper.pdf).
- Paszke, A., Gross, S., Massa, F., Lerer, A., Bradbury, J., Chanan, G., Killeen, T., Lin, Z., Gimelshein, N., Antiga, L., Desmaison, A., Köpf, A., Yang, E., DeVito, Z., Raison, M., Tejani, A., Chilamkurthy, S., Steiner, B., Fang, L., Bai, J., Chintala, S., 2019. PyTorch: An Imperative Style, High-Performance Deep Learning Library. *arXiv e-prints*, [arXiv:1912.01703](https://arxiv.org/abs/1912.01703)doi:[10.48550/arXiv.1912.01703](https://doi.org/10.48550/arXiv.1912.01703), [arXiv:1912.01703](https://arxiv.org/abs/1912.01703).
- Pedregosa, F., Varoquaux, G., Gramfort, A., Michel, V., Thirion, B., Grisel, O., Blondel, M., Müller, A., Nothman, J., Louppe, G., Prettenhofer, P., Weiss, R., Dubourg, V., Vanderplas, J., Passos, A., Cournapeau, D., Brucher, M., Perrot, M., Duchesnay, É., 2011. Scikit-learn: Machine Learning in Python. *Journal of Machine Learning Research* 12, 2825–2830. doi:[10.48550/arXiv.1201.0490](https://doi.org/10.48550/arXiv.1201.0490), [arXiv:1201.0490](https://arxiv.org/abs/1201.0490).
- Reid, M.D., Williamson, R.C., 2011. Information, divergence and risk for binary experiments. *Journal of Machine Learning Research* 12, 731–817. URL: <http://jmlr.org/papers/v12/reid11a.html>.
- Sadeh, I., Abdalla, F.B., Lahav, O., 2016. ANNz2: Photometric Redshift and Probability Distribution Function Estimation using Machine Learning. *Publications of the ASP* 128, 104502. doi:[10.1088/1538-3873/128/968/104502](https://doi.org/10.1088/1538-3873/128/968/104502), [arXiv:1507.00490](https://arxiv.org/abs/1507.00490).



Salvato, M., Ilbert, O., Hoyle, B., 2019. The many flavours of photometric redshifts. *Nature Astronomy* 3, 212–222. doi:[10.1038/s41550-018-0478-0](https://doi.org/10.1038/s41550-018-0478-0), [arXiv:1805.12574](https://arxiv.org/abs/1805.12574).

Schaap, W.E., van de Weygaert, R., 2000. Continuous fields and discrete samples: reconstruction through Delaunay tessellations. *Astronomy and Astrophysics* 363, L29–L32. doi:[10.48550/arXiv.astro-ph/0011007](https://doi.org/10.48550/arXiv.astro-ph/0011007), [arXiv:astro-ph/0011007](https://arxiv.org/abs/astro-ph/0011007).

Schuldt, S., Suyu, S.H., Cañameras, R., Taubenberger, S., Meinhardt, T., Leal-Taixé, L., Hsieh, B.C., 2021. Photometric redshift estimation with a convolutional neural network: NetZ. *Astronomy and Astrophysics* 651, A55. doi:[10.1051/0004-6361/202039945](https://doi.org/10.1051/0004-6361/202039945), [arXiv:2011.12312](https://arxiv.org/abs/2011.12312).

Sánchez, C., Carrasco Kind, M., Lin, H., Miquel, R., Abdalla, F.B., Amara, A., Banerji, M., Bonnett, C., Brunner, R., Capozzi, D., Carnero, A., Castander, F.J., da Costa, L.A.N., Cunha, C., Fausti, A., Gerdes, D., Greisel, N., Gschwend, J., Hartley, W., Jouvel, S., Lahav, O., Lima, M., Maia, M.A.G., Martí, P., Ogando, R.L.C., Ostrovski, F., Pellegrini, P., Rau, M.M., Sadeh, I., Seitz, S., Sevilla-Noarbe, I., Sypniewski, A., de Vicente, J., Abbot, T., Allam, S.S., Atlee, D., Bernstein, G., Bernstein, J.P., Buckley-Geer, E., Burke, D., Childress, M.J., Davis, T., DePoy, D.L., Dey, A., Desai, S., Diehl, H.T., Doel, P., Estrada, J., Evrard, A., Fernández, E., Finley, D., Flaugher, B., Frieman, J., Gaztanaga, E., Glazebrook, K., Honscheid, K., Kim, A., Kuehn, K., Kuropatkin, N., Lidman, C., Makler, M., Marshall, J.L., Nichol, R.C., Roodman, A., Sánchez, E., Santiago, B.X., Sako, M., Scalzo, R., Smith, R.C., Swanson, M.E.C., Tarle, G., Thomas, D., Tucker, D.L., Uddin, S.A., Valdés, F., Walker, A., Yuan, F., Zuntz, J., 2014. Photometric redshift analysis in the dark energy survey science verification data. *Monthly Notices of the Royal Astronomical Society* 445, 1482–1506. URL: <https://doi.org/10.1093/mnras/stu1836>, doi:[10.1093/mnras/stu1836](https://doi.org/10.1093/mnras/stu1836), [arXiv:https://academic.oup.com/mnras/article-pdf/445/2/1482/18197851/stu1836.pdf](https://academic.oup.com/mnras/article-pdf/445/2/1482/18197851/stu1836.pdf)